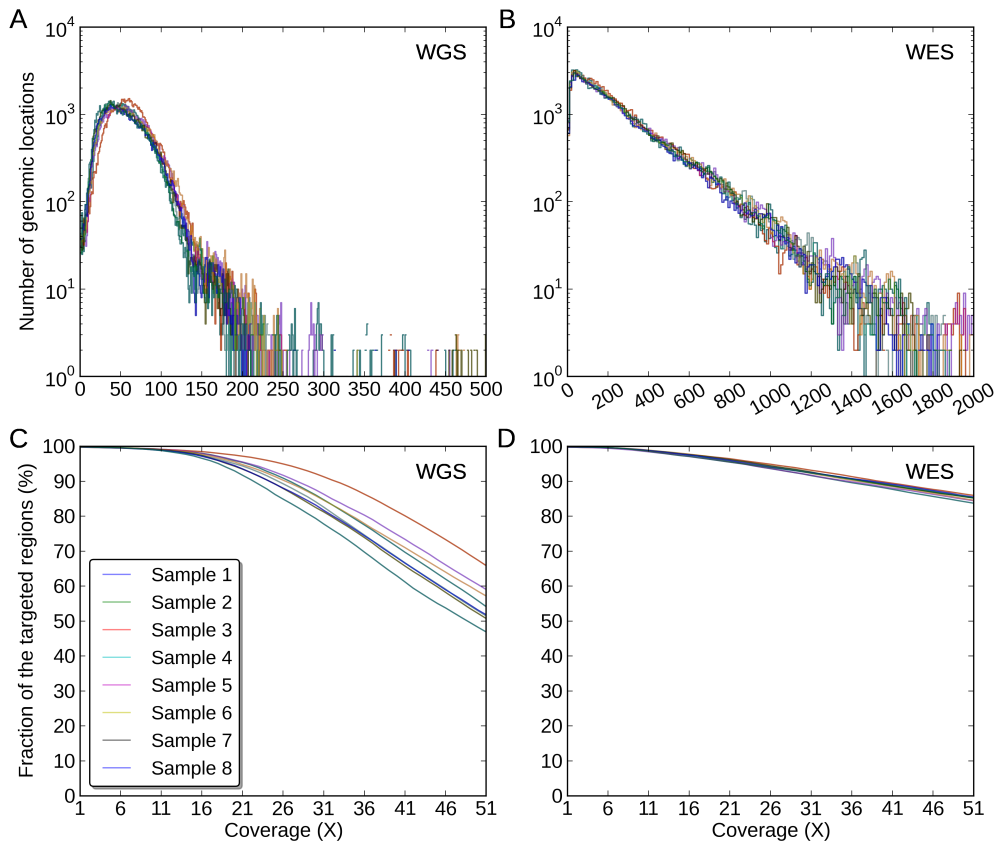


Additional Data File 1

Supplemental Figures

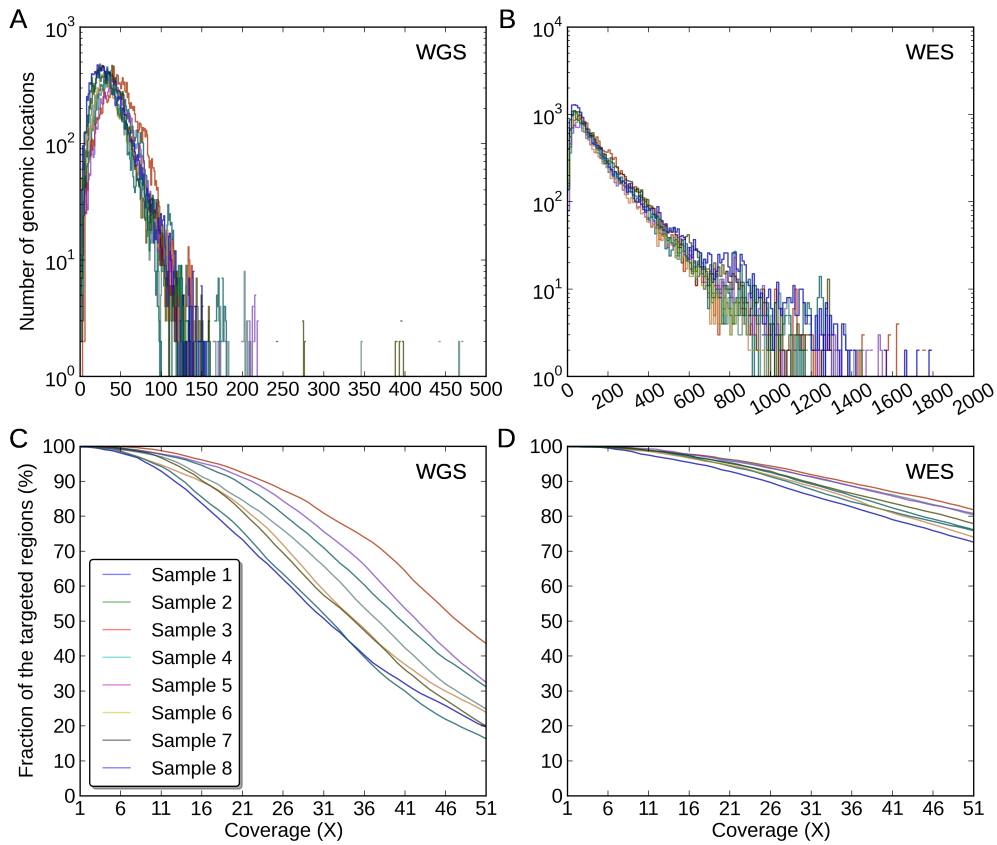
Supplemental Figure S1



Supplemental Figure S1. **Coverage distributions of the WGS-WES intersection**

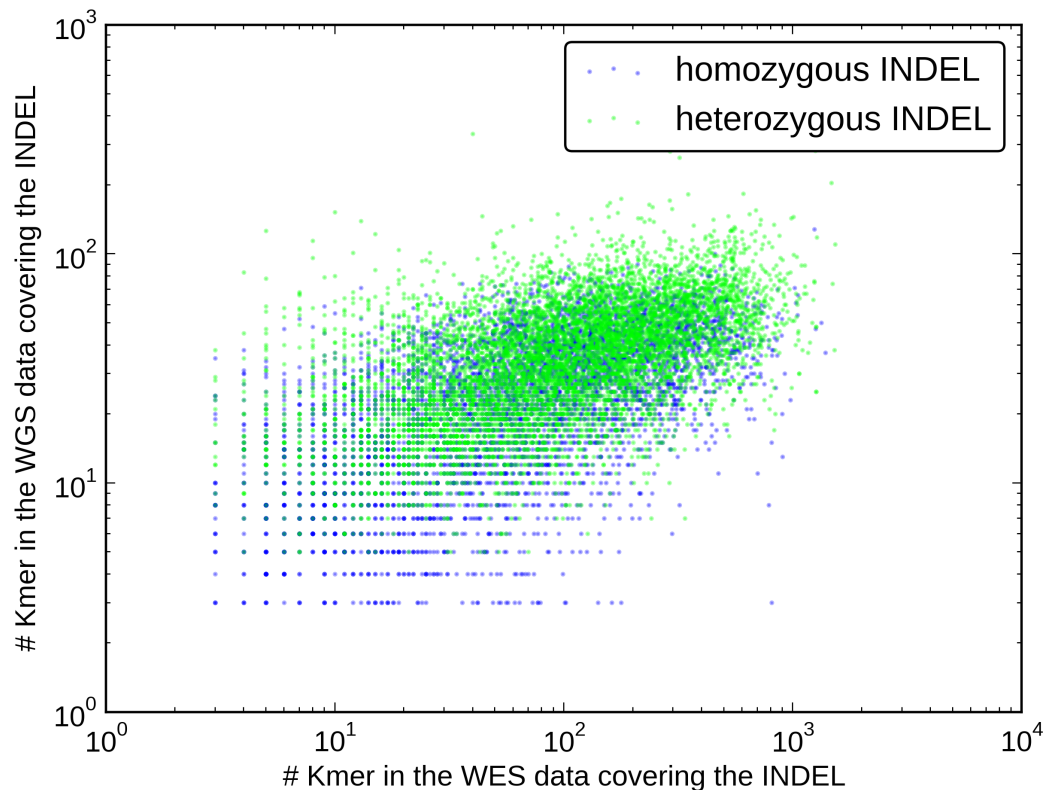
INDELs regions in (A) the WGS data, (B) the WES data. The Y-axis for A) and B) is of log10-scale. The coverage fractions of the WGS-WES intersection INDELs regions from 1X to 51X in (C) the WGS data, (D) the WES data.

Supplemental Figure S2



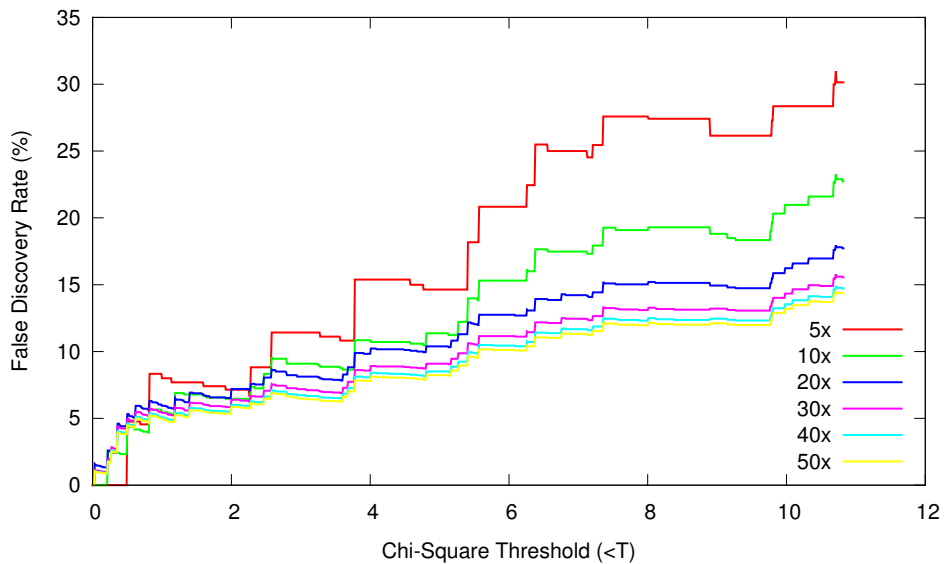
Supplemental Figure S2. **Coverage distributions of the WES-specific INDELS regions in (A) the WGS data, (B) the WES data.** The Y-axis for A) and B) is of log10-scale. The coverage fractions of the WES-specific INDELS regions from 1X to 51X in (C) the WGS data, (D) the WES data.

Supplemental Figure S3



Supplemental Figure S3. **Pair-wise base coverage relationship of INDEL called by both WGS and WES data.** These INDELS were partitioned by zygositys: homozygous (blue) and heterozygous INDELS (green). The X-axis shows the number of k-mer covering an INDEL in the WES data, and the Y-axis shows the number for WGS data.

Supplemental Figure S4



Supplemental Figure S4. **Characterization of the false discovery rate (FDR) based on validation data.** INDELs were partitioned based on k-mer coverage of the alternative allele and the INDEL Chi-Square scores. The X-axis shows Chi-Square scores of INDELs less than a certain threshold, and the Y-axis represents the FDR.

Supplemental Tables

Supplemental Table S1

Supplemental Table S1. **Mean depth coverage of WGS and WES data in different regions.** This table shows data corresponding to Figure 3, Figure 4, Supplemenatal Figure S1, and Supplemenatal Figure S2. The standard deviation is shown in parenthesis.

Mean coverage	Exonic targeted regions	WGS-WES intersection INDEL regions	WGS-specific INDEL regions	WES-specific INDEL regions
WGS	71X (3.3X)	58X (3.4X)	61X (2.9X)	41X (5.2X)
WES	337X (18.2X)	252X (7.0X)	137X (12.1X)	171X (10X)

Supplemental Table S2

Supplemental Table S2. **Mean coverage fractions of WGS and WES data in different regions.** This table shows data corresponding to Figure 3, Figure 4, Supplemenatal Figure S1, and Supplemenatal Figure S2. The standard deviation is shown in parenthesis.

	Coverage fraction	Exonic targeted regions	WGS-WES intersection INDEL regions	WGS-specific INDEL regions	WES-specific INDEL regions
WGS	1X	99.9% (0.1%)	99.8%(0.04%)	99.9% (0.03%)	99.9% (0.06%)
	20X	98.2% (0.2%)	96.0% (1.1%)	93.9% (1.4%)	86.9% (6.1%)
	50X	81.0% (3.1%)	57.5% (6.0%)	54.5% (0.4%)	29.4% (9.4%)
WES	1X	83.9% (1.1%)	99.8% (0.05%)	55.8% (0.3%)	99.9% (0.04%)
	20X	74.5% (0.1%)	96.6% (0.3%)	31.1% (2.1%)	96.0% (1.0%)
	50X	72.0% (0.3%)	85.7% (0.7%)	25.2% (3.7%)	78.7% (3.3%)

Supplemental Table S3

Supplemental Table S3. **Mean percentage and mean number of high quality, moderate quality, low quality INDELS in each call set.** This table shows data corresponding to Figure 5. The mean percentage and the mean number over eight

samples are shown in the upper and the lower of a cell, respectively. The standard deviation is shown in parenthesis.

	High quality	Moderate quality	Low quality
WGS-WES intersection INDELs	89% (0.7%)	9% (0.5%)	2% (0.5%)
	1454 (11.7)	148 (7.3)	31 (8.3)
WGS-specific INDELs	78% (1.4%)	15% (1.1%)	7% (1.6%)
	769 (13.9)	151 (10.7)	71 (15.8)
WES-specific INDELs	22% (3.4%)	37% (3.7%)	41% (3.3%)
	71 (11.2)	121 (11.9)	133 (10.9)

Supplemental Table S4

Supplemental Table S4. Mean percentages of high-quality INDELs partitioned by the following categories: homopolymer (A/C/G/T), other short tandem repeats (other STR), and non STR INDELs. This table shows data corresponding to Figure 6. The standard deviation is shown in parenthesis.

Regions	WGS-WES intersection INDELs	WGS-specific INDELs	WES-specific INDELs
Poly-A	11.2% (0.8%)	13.6% (0.6%)	24% (3.0%)
Poly-C	0.09% (0.06%)	0.3% (0.1%)	1.4% (1.0%)
Poly-G	0.3% (0.09%)	0.5% (0.1%)	0.6% (0.8%)
Poly-T	9.0% (0.6%)	7.9% (0.7%)	30% (3.5%)
Other STR	9.6% (0.5%)	11.1% (0.9%)	12.5% (3.1%)
Non-STR	70% (1.2%)	67% (1.1%)	31.9% (6.1%)

Supplemental Table S5

Supplemental Table S5. Mean fractions of low-quality INDELs partitioned by the following categories: homopolymer (A/C/G/T), other short tandem repeats (other STR), and non STR INDELs. This table shows data corresponding to Figure 6. The standard deviation is shown in parenthesis.

Regions	WGS-WES intersection INDELs	WGS-specific INDELs	WES-specific INDELs
Poly-A	19.6% (12.5%)	26.1% (7.0%)	41.5% (3.2%)
Poly-C	0.6% (1.6%)	0% (0%)	0.3% (0.3%)
Poly-G	0%	0.4% (0.09%)	0.3% (0.3%)
Poly-T	24.6% (11.2%)	19.0% (5.6%)	41.1% (3.5%)
Other STR	21.0% (7.3%)	11.9% (3.8%)	6.2% (1.2%)

Non-STR	34.1% (14.1%)	42.6% (9.4%)	10.7% (2.5%)
----------------	---------------	--------------	--------------

Supplemental Table S6

Supplemental Table S6. Number of INDELS in the WGS and WES data with multiple signatures partitioned by the following categories: homopolymer (A/C/G/T), other short tandem repeats (other STR), and non STR INDELS. This table shows data corresponding to Figure 7. The standard deviation is shown in parenthesis.

Regions	WGS	WES
Poly-A	25 (5.7)	35 (6.0)
Poly-C	0.3 (0.4)	1 (0.3)
Poly-G	0.6 (0.5)	0.8 (0.7)
Poly-T	16 (4.0)	36 (5.3)
Other STR	25 (4.8)	24 (3.4)
Non-STR	9 (2.6)	6 (1.4)

Supplemental Table S7

Supplemental Table S7. Number of reads in the following four regions: Exonic targeted regions, WGS-WES intersection INDEL regions, WGS-specific INDEL regions, WES-specific INDEL regions.

Number of reads	Exonic targeted regions	WGS-WES intersection INDEL regions	WGS-specific INDEL regions	WES-specific INDEL regions
WGS	241984	49008	26417	1775
WES	815945	205698	44346	11251

Supplemental Table S8

Supplemental Table S8. Probabilities of seeing k or more INDELS in a given family assuming a binomial distribution. Here we assumed a binomial distribution of the de novo exonic INDELS in the 343 SSC families.

Number of INDELS	= 0	≥ 1	≥ 2
Probability	0.78	0.22	0.03

Number of INDELs	≥ 3	≥ 4	≥ 5
Probability	0.0020	0.0001	0.000005

Supplemental Table S9

Supplemental Table S9. **Putative *de novo* exonic INDELs in these two families before and after applying filtering critiria.** The number of INDELs within regions of homopolymer A (poly-A), homopolymer T (poly-T), and microsatellites (ms) are shown in the parenthesis.

Putative <i>de novo</i>	WGS (poly-A, poly-T, ms)	WES (poly-A, poly-T, ms)	WGS (After filtering)	WES (After filtering)
Family 1	45 (27,14,4)	5 (3,1,1)	0	0
Family 2	49 (24,22,3)	17 (8,5,4)	0	0

Supplemental Note 1

Analysis of the effect of new filtering criteria on *de novo* INDEL calls

The two families in this study were previously reported in a population-scale autism study, with Sanger validation of *de novo* calls [1]. We used the *de novo* mode of Scalpel to identify *de novo* INDELs in these two families again, resulting in one *de novo* call set for WGS data and another *de novo* call set for WES data per family. We partitioned each call set by regions and filtered out the low quality INDELs. Iossifov *et.al* 2012 reported a total of N=85 *de novo* exonic INDELs in 343 families, i.e. there was 0.1 *de novo* exonic INDEL per child [1]. If we assume a binomial distribution of the *de novo* exonic INDELs with an equal chance ($p=1/343$), the probability of seeing at least X *de novo* exonic INDELs in a given family in this study can be computed as below:

$$P(X \geq k \text{ INDELs}) = 1 - \sum_0^k P(X = k - 1) = 1 - \sum_0^{k-1} \binom{N}{X} p^X q^{N-X}$$

where $P(X \geq k)$ is the probability of a given family having k or more *de novo* INDELs; N is the total number of exonic *de novo* INDELs reported, i.e. N=85; p is the probability of a hit on a given trial, i.e $p=1/343$; $q=1-p$.

Applications of using filtering criteria to reduce false positive *de novo* INDELs

Supplemental Table S8 shows the probabilities of seeing more than K INDELs from one of the 343 families reported in Iossifov *et al.* 2012 [1]. Scalpel has a *de novo* analysis mode; it could re-assemble each region associated with the candidate INDELs across the family members using a more sensitive parameter setting. This setting was indeed more sensitive for detecting *de novo* INDELs than single-sample calling. Due to this, we used the following more rigorous filtering criteria than the above assessment to exclude any

spurious false-positive de novo INDELs: coverage of the alternative allele >10 and Chi-Square score <4. Supplemental Table S9 showed the number of putative de novo INDELs in two families before and after applying this filtering criteria. All of the spurious *de novo* variants in the two families were successfully excluded, which was consistent with the validated results in the variant database reported by Iossifov *et al.* 2012 [1]. We noticed that, in both families, the majority of these false-positive de novo INDELs were poly-A/T relevant (91% for WGS, 78% for WES), which was consistent with the above assessment. This suggested that if we used very sensitive callers, we should control for poly-A/T false-positive de novo INDELs by applying a more rigorous filtering criteria, especially in population-scale sequencing projects, where there is substantial expense with experimental validation.

References:

1. Iossifov I, Ronemus M, Levy D, Wang Z, Hakker I, Rosenbaum J, Yamrom B, Lee YH, Narzisi G, Leotta A, et al: **De novo gene disruptions in children on the autistic spectrum.** *Neuron* 2012, **74**:285-299.